Toxicological evaluation of highly water dispersible few-layer graphene in vivo

Amalia Ruiz, Matteo Andrea Lucherelli, Diane Murera, Delphine Lamon, Cécilia Ménard-Moyon, Alberto Bianco

Toxicological evaluation of highly water dispersible few-layer graphene *in vivo*

Amalia Ruiz[‡], *Matteo Andrea Lucherelli*, *Diane Murera*, *Delphine Lamon*, *Cécilia Ménard-Moyon*, *Alberto Bianco*[*]

CNRS, Immunology, Immunopathology and Therapeutic Chemistry, UPR 3572, ISIS, University of Strasbourg, 67000 Strasbourg, France.

[‡]Present address: School of Pharmacy, Queen's University Belfast, 97 Lisburn Rd, Belfast BT9 7BL, UK.

[*]Correspondence: a.bianco@ibmc-cnrs.unistra.fr

Keywords: Carbon nanomaterials, intravenous injection, blood parameters, immune cells, biodistribution

Abstract

In the last decade, graphene-based materials have received increasing attention for both academic research and industrial uses. However, products containing graphene must meet the same standards for quality, safety and efficacy as products not containing nanomaterials. Our aim is to shed light on the toxicological characterization of few-layer graphene (FLG) dispersions. In the present study, graphene was easily dispersed in water using biocompatible riboflavin-5′-phosphate sodium salt (Rib). A highly concentrated FLG dispersion (G-Rib) was stable for months. G-Rib suspension was characterized by HR-TEM, Raman spectroscopy and ζ-potential. Our results showed that even at high concentration of G-Rib, cell survival was always above 85%. Then, we investigated the tissue distribution and toxic effects of G-Rib in mice up to 30 days after intravenous injections. Histological analysis of the tissues revealed hepatic accumulation and excretion through the kidneys. The biochemical and hematological parameters remained within the reference range showing no hematotoxicity. Finally, no signs of inflammation were detected in the cells isolated from the lymph nodes and spleen. The results of the study show that highly water dispersed FLG is a material with a very low toxic profile, which is one of the first requirements for the future development of biomedical applications.

1. Introduction

Graphene is very often used to refer to a family of materials including single-layer graphene (G), few-layer graphene (FLG), graphene oxide (GO), and reduced graphene oxide (rGO). Graphene members are extensively studied nowadays for their potential in biomedical and (bio)technological applications.[1] Their unique and fascinating mechanical and thermal properties make them ideal candidates for the development of flexible and robust devices, composites or implants.[2] The electronic properties of graphene are also studied to act as conducting components, electrodes or support in electronic devices.[3] The possibility to functionalize the surface shows promising results in the development of drug delivery carriers with precise control of the amount of drug and the release profile.[4,5] However, drug products containing nanomaterials must meet the same standards for quality, safety and efficacy as for drug products not containing nanomaterials. Consequently, many research efforts are focused on the assessment of the toxicity of graphene-based nanomaterials.[6–8]

Another challenge in the use of G in bioapplications is to modulate its hydrophobic surface. Unfortunately, the dispersibility of graphene and its derivatives is almost inversely proportional to its hydrophobic properties (hydrophilicity: GO > rGO > G~FLG). Chemical functionalization of these materials can improve their dispersibility,[9] but can also increase their defectiveness and have a negative impact on their properties. Additionally, a desirable G dispersion in aqueous media for biological applications should have a long shelf life or be easily re-dispersible. There is also a need for highly concentrated dispersions of graphene, particularly in water, not only to reduce costs and risks of transporting and storing large diluted solutions in the pharmaceutical industry, but also to provide to end users the possibility to dilute the dispersions in their own formulations.

In recent years, different articles showed *in vivo* assessment of many graphene derivatives.[6] Most of the studies were carried out using GO. In general, experiments were focused on the toxicity of graphene derivatives in the lungs, liver, kidney and spleen.[10,11] The common administration routes were inhalation or instillation for airway exposure studies,[12] oral for gastrointestinal tract absorption or intraperitoneal[13] or intravenous administration.[11]

In contrast, the *in vitro* and *in vivo* toxicological characterization of G and FLG dispersions have been poorly studied.[7] One of the first studies showed that inhaled graphene nanoplatelets, up to 25 µm in lateral size, deposited in the lungs, causing frustrated phagocytosis and inflammation.[14] In a similar study, intratracheal instillation of thinner (~10

layers) and smaller (2 μm lateral size) graphene nanoplatelets into the lungs was monitored for up to 3 months, showing slow clearance and disturbance of the immunological and physiological homeostasis of treated mice.[15] Intratracheally inhaled FLG with a smaller lateral size (up to 1.25 μm) still persisted in the lungs up to 28 days after exposure, provoking instead only transient pulmonary effects.[12] More recently, graphene nanoplatelets, forming agglomerates of more than 4 μm in size, showed a dose-dependent toxicity leading to high levels of reactive oxygen species (ROS) and depletion of mitochondrial membrane potential.[16] These results are in agreement with the study of Pelin *et al.* using FLG on skin cells.[17]

Most of the studies involved very thick and large graphene sheets. As already mentioned above, there is a strong need for highly stable suspensions of G and FLG in water, which are likely to have a different impact once exposed to a living organism. Ayán-Varela et al., were the first to demonstrate the potential use of riboflavin to prepare highly concentrated dispersions of FLG in water.[18] However, this study focuses on the expedite preparation of a material with high catalytic activity in the reduction of nitroarenes and good performance as electrocatalyst toward the oxygen reduction reaction. Riboflavin is an essential water-soluble vitamin involved in different biological functions such as transporter specific cell internalization, implication in redox reactions, fluorescence and photosensitizing. For these reasons, researchers of various fields, from targeted drug delivery and tissue engineering to optoelectronics and biosensors, have attempted the functionalization of different nano-objects with this vitamin.[19] Furthermore, tumor cells exhibit increased riboflavin metabolism as compared to normal cells and when riboflavin have been conjugated to ultrasmall iron oxide nanoparticles, polyethylene glycol polymers, dendrimers, and liposomes, they have shown a high affinity towards tumors in preclinical studies.[20] Since graphene related materials are proposed as a prospective platform for therapeutics including cancer therapy, it could be sensible to provide an overview on the toxicological profile of these materials.

In the present work, we report a comprehensive toxicological study of the material, which, in our opinion, is considered to be essential in a nanobiotechnological scenario. We sought to understand how FLG exfoliation with this biocompatible molecule affects the physicochemical properties (e.g. size, number of layers, stability in aqueous media) and its toxicological impact *in vitro* and *in vivo*. Therefore, it was essential to characterize the toxicity using a combination of *in vitro* cell culture models and an *in vivo* murine model, where the FLG was administered intravenously at a low and a high dose. In summary, this study provides insights on how FLG

exfoliated with a biocompatible molecule like riboflavin impacts on immune cells from the reticuloendothelial system and biochemical and hematological parameters after 30 days.

2. Materials and Methods

2.1. Synthesis and characterization

Graphite (LOT #BCBS5850V) powder (< 20 μm) and riboflavin-5′-phosphate sodium salt (Rib) were purchased from Sigma-Aldrich. MilliQ water, purified using a Millipore filter system MilliQ® and free endotoxin Polisseur Biopak®, was used for the preparation of the solutions. Sonication bath Elma model Elmasonic P was used for the exfoliation of graphite. Omnipore polytetrafluoroethylene membrane filters 0.1 μm were used for the filtration of all dispersions of graphene. The centrifugation of the dispersions was performed using a Beckman Avant J-25 centrifuge. The lateral size dimension was measured using a Hitachi 7500 transmission electron microscope (Hitachi High Technologies Corporation, Tokyo, Japan) equipped with an AMT Hamamatsu digital camera (Hamamatsu Photonics, Hamamatsu City, Japan). High resolution TEM (HR-TEM) and selected area electron diffraction (SAED) analyses were performed on a JEOL 2100F TEM/STEM electron microscope operating at 200 kV. ζ-potential was evaluated using a high-performance particle sizer (HPPS) from Malvern.

2.2. Graphene production

Exfoliation of graphene was carried out directly in water using 1.5 g of graphite dispersed in 200 mL of a solution of Rib at 1 mg/mL.[18] The solution was sonicated at 37 MHz for 5 hours at temperature < 30°C by the replacement of warm water with ice every 30 min. After sonication, the dispersion was centrifuged at 1500 g for 1 h to recover the most stable sheets. The supernatant containing the exfoliated layers of graphene was collected, filtered and washed with 300 mL of water to remove the excess of Rib. The powder was then sonicated for 5 min in 20 mL of MilliQ water obtaining the final graphene aqueous dispersion (G-Rib).

2.3. Cellular studies

2.3.1. *Cell culture.*

HeLa (epithelial, human cervical adenocarcinoma) and RAW 264.7 (macrophages, Abelson murine leukemia virus-induced tumor) cells were cultured as mono-layers in Dulbecco's modified Eagle medium supplemented with 10 μg/mL gentamycin (Lonza BioWhittaker), 10 mM HEPES (Lonza BioWhittaker), 0.05 mM β-mercaptoethanol (Lonza BioWhittaker) and 10 % FCS, in a humidified incubator (37°C, 5% CO_2). For the toxicity experiments, cells were seeded in 24-well plates (approximately 1×10^5 cells/well, 1 mL/well). The cells were left to grow until 70-80% confluency and exposed for up to 24 hours to G-Rib. G-Rib was diluted in

the cell culture medium at different concentrations and subsequently the cells were exposed for 24 h.

2.3.2. *Cytotoxicity assay.*

Cell viability was determined by flow cytometry using the standard assay with FVD (Fixable Viability Dyes) 24 h after exposure to the materials. Cells were detached from the plates using a scraper in the case of RAW 264.7, and for HeLa cells a solution of 0.25% trypsin/0.53 mM EDTA was used. Supernatants were always pooled in order to avoid the loss of non-attached cells. The cells were washed with PBS, 2% fetal calf serum and then were incubated (20 min, 4°C) with the dye (dilution 1:2000). Thereafter, cells were washed with PBS, 2% FCS and resuspended in 300 µL and immediately acquired on the cytometer. At least 10,000 cells were counted for each sample and experiments were performed in triplicate.

2.3.3. *Data analysis and statistical methods.*

Flow cytometry data were saved as LMD files and subsequently analyzed using FlowJo software (FlowJo LLC, software version 7.6.5. Ashland, OR, USA). Cell viability (%) was calculated as $[(A - B)/A \times 100]$, where A and B are the number of dead cells of control and treated cells, respectively. Values represent mean ± SD (n = 3). Two-way analysis of variance (ANOVA) and Bonferroni's multiple comparisons test were adopted for statistical significance ($p<0.05$).

2.4. Animal studies

2.4.1. *General toxicity.*

Toxicological characterization of exfoliated graphene after a single intravenous administration was performed in a murine model (BALB/c mice, 11-13 weeks, 18-20 g, n=5/group). Mice were housed in the IBMC animal facility (agreement number G67-482-2). They were maintained under controlled conditions before and during the experiments (*i.e.*, room temperature at 25°C; relative humidity of 65%; 12 h light/dark cycle). Access to food and water was provided *ad libitum*. All experiments were carried out in conformity with the 2010/63/UE European animal bioethics legislation (French decree #2013-118 – 1st February 2013) and were approved by the Regional Ethics Committee of Strasbourg (CREMEAS) and by the French Ministry of Higher Education and Research (APAFIS#3280-2015121815099907 v2). An acute toxicity assay was performed using exfoliated graphene at two dose levels: 5 and 15 mg/kg body weight (injections of 100 and 300 µg/mouse, respectively). After a single intravenous

injection of graphene suspensions in a 5% dextrose solution, clinical observations were performed daily for up to 30 days. Animals were terminated at 24 h, 14 days, and 30 days after injection and liver, kidneys, and spleen were collected for analysis. After extraction, the organs were fixed in 10% paraformaldehyde and embedded in paraffin blocks. Sections of 8 µm were deparaffinized and rehydrated before staining. Hematoxylin and eosin staining was used for the determination of histopathological changes in the tissue. Blood was collected in EDTA (10%) and analyzed using a cell counter. The biochemical and hematological analyses were performed at the Mouse Clinical Institute (MCI, Illkirch, France).

2.4.2. *HR-TEM of the urine.*

A urine sample was dialyzed against MilliQ water using a 300,000 MWCO dialysis membrane (Spectrum Laboratories, Inc.) and lyophilized. The solid was dispersed in MilliQ water and deposited on a TEM grid made of a holey carbon membrane of 10 nm thickness on copper grids, and then dried under a lamp. HR-TEM and SAED analyses were performed on a JEOL 2100F TEM/STEM electron microscope operating at 200 kV.

2.4.3. *Immunofluorescence staining.*

The following antibodies purchased from BD Bioscience (BD) (Le Pont-De-Claix, France) or Biolegend (Bio) (Fell, Germany) were used to stain the cells: fluorescein isothiocyanate (FITC) labelled anti-mouse CD3 (clone 145-2C11, BD 553062), peridinin-chlorophyll proteins (PerCp)-Cyanin 5.5 (Cy5.5) labelled anti-mouse CD3 (clone 145-2C11, 45-0031-82 eBio), PerCp-Cy5.5 labelled anti-mouse CD11b, allophycocyanin (APC) labelled anti-mouse CD11b, FITC labelled anti-mouse CD19, PerCP-Cy5.5 labelled anti-mouse CD19 (clone ID3, 551001), phycoerythrin (PE)-Cyanin7 (Cy7) labelled anti-mouse CD44 (clone IM7, 103030, Bio), PE labelled anti-mouse CD69 (clone H1.2F3, 553237, BD), PE labelled anti-mouse CD86 (clone GLI, 553692, BD), APC labelled anti mouse, APC-Cy7 labelled anti-mouse TCRβ (clone H57-597, 560656, BD) and the fixable viability dye (FVD) eflour 450 (65-0863-18, eBioscience).

3. Results and discussion

3.1. **Exfoliated graphene synthesis and characterization.**

Direct exfoliation of graphene in water requires the use of surfactants due to its hydrophobic surface.[21] One of the most popular methods to obtain stable graphene water dispersions is

the use of mechanical forces like sonication in presence of surfactants, which are able to intercalate between graphene sheets and increase the layer distance on graphite, enhancing the exfoliation process.[22] For the biological applications of graphene it is mandatory to use non-toxic molecules capable of producing high concentrations of graphene.[23] In this study, we used as the exfoliating agent the sodium salt of riboflavin-5′-phosphate, a derivative of vitamin B2, because of its biocompatibility and high capacity to stabilize graphene aqueous dispersions.[18] Graphene was produced directly in water by bath sonication of graphite in a solution of Rib. Steps of ultracentrifugation and filtration were applied to isolate the most stable sheets and remove the excess of Rib. A highly concentrated G-Rib dispersion (2 mg/mL) was obtained, with a production yield of ~2.5 *wt.* percentage. This was stable for months without the formation of eye-visible agglomerates and precipitates. The suspension of the exfoliated graphene was then characterized using different complementary analytical and microscopic techniques. TEM micrographs showed individual sheets with an average size of ~840 nm (Figure 1A). The lateral size distribution was calculated from TEM images by measuring at least 300 sheets of graphene. The histogram of this distribution, with values ranging between 200 and 1800 nm, shows that the total amount of particles with lateral dimension > 1000 μm is lower than the 11% (Figure 1B). To further elucidate the state of aggregation of G-Rib in the dispersion, HR-TEM micrographs were used to calculate the number of layers on G-Rib sheets (Figure 1C). Interestingly, an average of 5 layers per sheet was observed for ~70% of the sheets, confirming the few-layer nature of the material (Figure 1D).[24] This result is consistent with other previous studies that reported the successful exfoliation of graphene in water.[21,25] Furthermore, Raman spectroscopy showed a small increase in defects in comparison with starting graphite (Figure 1E, red line), with an average I_D/I_G ratio for the sheets of ~0.28 (black line). Because it is important for further biological investigations, we evaluated the stability of the dispersion at different pH by ζ-potential measurements. High stability of the sheets between pH 4 and 12 was observed. In this range of pH, the material showed a strong negative surface charge (-40 to -50 mV) thanks to the phosphate group of Rib, which is indicative of a colloidal suspension suitable for carrying out different tests in a biological environment (Figure 1F).

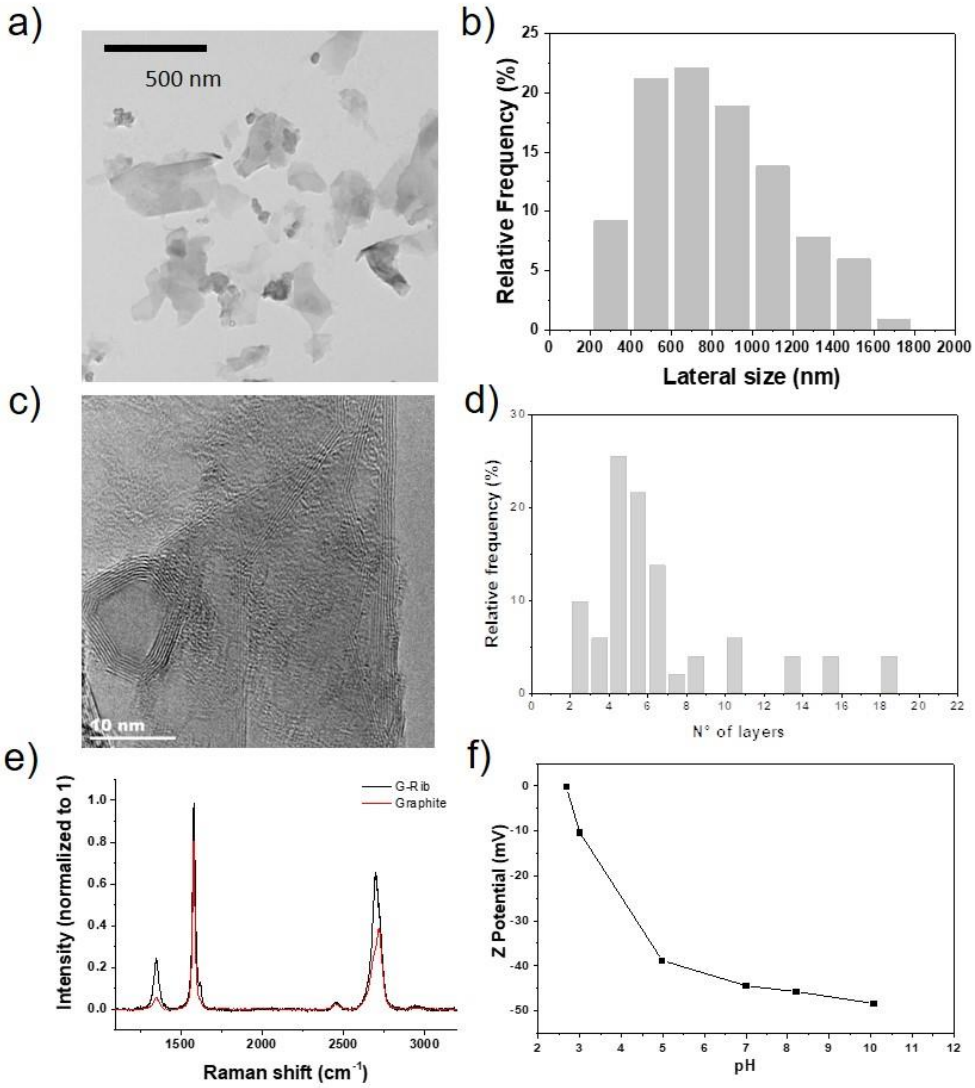

Figure 1. A) TEM image of representative G-Rib sheets. B) Histogram of lateral size distribution of G-Rib sheets by TEM. C) HR-TEM image of G-Rib. D) Histogram of the number of layers evaluated, observing more than 50 particles by HR-TEM. E) Raman spectra of G-Rib (black line) and of starting graphite (red line). F) Evolution of ζ-potential of an aqueous dispersion of G-Rib (conc. 100 µg/mL) with the pH.

The amount of riboflavin adsorbed onto the graphene surface was calculated from the percentage of nitrogen measured by elemental analysis. Surprisingly, the result showed that the dispersion of G-Rib contains 7% weight of riboflavin, corresponding to roughly 1.9×10^{-4} mol/g, a lower amount compared with other studies reporting the surfactant-assisted exfoliation of graphite.[26] Considering that the theoretical area available in a monolayer of graphene is 2630 m^2/g, using as a reference a sheet with a lateral size of 1 µm,[27] we were able to calculate

the approximate amount and distribution of the surfactant onto the graphene surface. Since the vitamin can interact with both sides of the graphene sheets, we estimated that ~30% of graphene surface is involved in the interaction with the surfactant. This is an interesting result that allows further functionalization of the nanomaterial with other biomolecules, drugs or active agents. The loading capacity of graphene-based carriers has been extensively studied and depending on the molecule it can go up to 300% (wt.%).[28]

3.2. ***In vitro*** **studies**

The *in vitro* toxicological evaluation of a new material is an important aspect of research, especially when aimed at biomedical applications. Cytotoxicity of nanomaterials, and particularly the graphene family, is a complex field. Recent publications highlight the importance of testing toxicity on endothelial cells, which act as the first contact and barrier for nanomaterials entering circulation. Moreover, oxidative stress and inflammation induced by nanomaterials have been suggested as the mechanisms associated with their toxicity to endothelial cells. Dysfunction of autophagy (excessive autophagy induction) has also been suggested as one of the mechanisms associated with the toxicity of NPs to human ECs.[29] Recently, a comprehensive study has been published demonstrating how FLG does not affect the function and the autophagic activity of primary lymphocytes.[30] The results showed that FLG neither impacts the viability and activation of T and B cells nor their autophagic activity. Similar results shed light on the impact of FLG on primary macrophages and show that FLG does not elicit immunological responses leading to cell death.[31] On the other hand, the use of immortalized cell lines is a commonly used model for toxicological evaluation of nanomaterials. Liao et al., summarizes important work about the interactions of graphene-based materials with these cells: e.g. uptake process, interaction with the cell membrane, mechanisms of toxicity, etc; where HeLa cells and RAW 264.7 macrophages have been frequently used.[32]

Before studying the effects of G-Rib in an animal model, we wanted to evaluate the cytotoxic effects in two different cell lines. The cytotoxicity of the material was evaluated through the degree of cell survival by flow cytometry using the standard assay with violet FVD (Figure 2A, D). We used HeLa cells as both non-phagocytic epithelial and cancer cell model and RAW 264.7 macrophages as immune and phagocytic cell model. Interestingly, after a 24-hour incubation with G-Rib up to 300 µg/mL, the cells showed practically no toxicity as per the

survival rate. We observed that G-Rib was slightly less toxic for RAW 264.7 macrophages compared to HeLa cells. Pursuant to ISO 10993-5, percentages of cell viability above 80% are considered as non-cytotoxicity; within 80%–60% weak; 60%–40% moderate and below 40% strong cytotoxicity respectively.[33] Overall, values of survival were always above 85% for the nanomaterial, hence it could be considered as non-toxic. A solution containing the same percentage of Rib was used as a control to assess if there was a possible impact of the surfactant in the cell viability. As expected, this natural molecule had no significant effect on both cell lines. Bright field microscopy showed that G-Rib uptake after 24 hours did not affect cell adherence and morphology compared to the control (Figure 2B, C, E and F). Interestingly, RAW 264.7 macrophages showed a higher uptake of the material compared with HeLa cells due to their phagocytic nature.

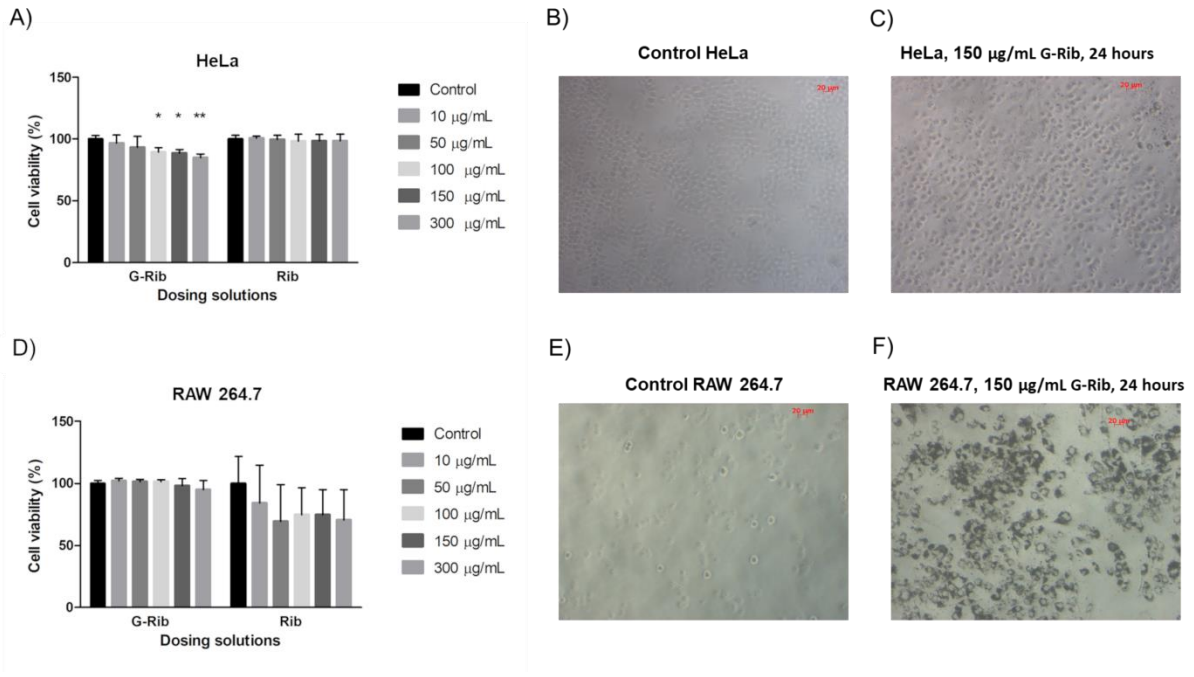

Figure 2. *In vitro* toxicological characterization. Cell viability after 24 hours of incubation was evaluated by flow cytometry using the standard assay with violet FVD. (A) HeLa cells; (D) RAW 264.7 cells. The cells were treated with G-Rib, and a solution of Rib at equivalent concentration was used as control. The data shown represents the mean ± SD (n = 3 of 3 independent experiments). Two-way ANOVA followed by Bonferroni's post-test: ns $p>0.05$, *$p<0.05$, **$p<0.01$ was used for statistical analysis. Cells were visualized by optical microscopy (bright field) 24 hours after incubation with the material. (B) HeLa cells control,

(C) HeLa cells treated with G-Rib at 150 µg/mL, (E) RAW 264.7 cells control, (F) RAW 264.7 cells treated with G-Rib at 150 µg/mL.

Most of the studies exploring graphene-based candidates for biomedical applications focus on the use of GO because of its higher hydrophilicity compared with graphene.[34–36] Only a few articles have evaluated the toxicity of graphene and depending on the cell line used a significant decrease (up to 50%) in cell viability was observed after incubation with 25 µg/mL of nanomaterial in the cell culture medium.[37,38] In these cases, the authors postulate that the poor dispersibility of the material in biological media provoked the agglomeration and accumulation of graphene on the cell membrane, which greatly hindered the uptake of essential nutrients and proteins, and blocked calcium ion channels, leading to intracellular stress. In RAW 264.7 cells, Li *et. al* demonstrated that graphene can induce cytotoxicity (~78% cell death was observed at 100 µg/mL treatment concentration) through the depletion of mitochondrial membrane potential resulting in the increase of ROS leading to the activation of MAPK and TGF-β that in turn activated caspase-3 and PARP proteins resulting in apoptosis.[39] A comparable cytotoxicological study with other graphene-based materials like GO and GO functionalized with quantum dots in HeLa and RAW 264.7 cells has been carried out.[9] Whilst the materials were not harmful for HeLa, RAW 264.7 resulted in a more sensitive cell line with a drop in toxicity to 40%. These results suggest that graphene exfoliation in the presence of riboflavin could improve the biocompatibility of the nanomaterial. Riboflavin likely alleviates graphene cytotoxicity as it facilitates a high dispersibility and stability in aqueous media, avoiding agglomeration onto the cell surface and the consequent damage of the membranes. Special significance is the result obtained with RAW 264.7 macrophages, which are more sensitive than epithelial cells and usually show higher *in vitro* toxicity when nanomaterials are tested.[9,40] However, further studies are required to understand G-Rib biointeractions with cells in terms of uptake, intracellular trafficking, mechanisms of biodegradation and possible impact in cytotoxicity in a longer term.

3.3. *In vivo* studies

After demonstrating that G-Rib does not affect cell viability at very high doses, we decided to study the effects *in vivo* in a murine model. A crucial step in the toxicological evaluation of graphene-based materials is their dose- and/or time-dependent safety pharmacological assessment in animal models under various modes of administration (e.g. intravenous, intraperitoneal, or oral). In the case of graphene-related materials most studies have been

carried out using GO or graphene functionalized with polymers to enhance its biocompatibility, avoiding the formation of aggregates leading to undesired side effects.[36] Only a few studies have been carried out analyzing the toxicological effects of FLG. For instance, a complex of graphene with 2% Pluronic in water was evaluated for pulmonary toxicity. Inflammation, apoptosis, increase of mitochondrial respiration and pulmonary inflammation were observed in the lungs of the mice.[41] Another study described how graphene was able to induce the development of the local inflammatory reaction and the development of granulomas in parenchymal organs.[42] From a careful review of the literature we found important differences across dosing concentrations used in *in vivo* toxicological studies of graphene-based materials. We identified two ranges of concentrations in different studies: from 1 to 20 mg/kg [43–48] and from 50 to 500 mg/kg [49–51]. We believe that public health risk assessments for nanomaterials must evaluate realistic doses in order to draw meaningful conclusions from both in vitro and in vivo studies. Although exposure of high doses of graphene-based materials can lead to a rapid detection and quantification of the unsafe threshold, the main public health concern related to nanomaterials should refer to chronic low-dose exposures and asses on future studies longer exposure times.

3.4. General toxicity and biodistribution

We have evaluated the biological impact of G-Rib after a single intravenous (i.v.) administration in Balb/c mice. G-Rib was injected intravenously at two dose levels: 5 mg/kg (~100 µg/mouse) and 15 mg/kg (~300 µg/mouse) body weight. Clinical observations were performed daily for up to 30 days. The experiments concluded with a 100% rate of survival, and no general signs of toxicity (*e.g.* seizures, disheveled hair, irregular respiration, gastrointestinal symptoms, immobility, convulsions, severe decubitus paralysis or death) or dose-related effects were observed. Body weight of the animals did not drop below 5% from the start to the end of the study. Immediately after the animals were euthanized, organs were harvested and immersed in PBS to remove any excess of blood for their macroscopic evaluation. No pathological changes were seen during this observation. To our surprise the color of the liver, kidneys, lungs and spleen retained their normal color without changes compared to the control. This observation contrasts with other studies that used 4 mg/kg of bodyweight of GO, Graphite or Diamond in a rat model, showing noticeable accumulation in the stomach serous membrane, between the connective tissues of the abdominal skin, muscles, and peritoneum, in abdominal lipid tissue, and in organs like the liver or the spleen.[52] Organs of mice were collected for hematoxylin and eosin (H&E) staining and histological examination.

The liver accumulation has been considered as one of the major obstacles of nanomedicine delivery. The liver is the main organ responsible for the detoxification of metabolites and the clearance of exogenous compounds. In the liver tissue, blood plasma freely passes through the fenestrations into the perisinusoidal space, where the voluminous membrane of hepatocytes acts to remove blood components and nutrients for storage and processing. Within the liver microarchitecture, blood flow is significantly slower than in the systemic circulation. This reduced flow promotes preferential nanomaterial accumulation within the sinusoid and the nanomaterials will then have increased probabilities of clearance by the cells.[53] Ultimately, nanomaterials are cleared primarily by Kupffer cells, endothelial cells, B cells, etc. Nanomaterials that are not taken up, leave the organ through the central vein, re-joining the systemic circulation and may return to the liver during a subsequent pass. In this way, it´s important to characterize the clearance process in the long term. Sasidharan et. al., have reported the long term hepatic toxicity of FLG synthesized using an arc discharge method.[43] Swiss albino mice were intravenously injected with a single dose of 20 mg/kg. In agreement with our results, FLG treated animals showed large numbers of Kupffer cells that engulfed graphene in the liver. However, the authors describe inflammatory changes such as portal congestion, occasional sinusoidal congestion and severe degeneration in hepatocytes after 90 days.

For mice i.v. injected with G-Rib, large brown areas were observed in the liver (Figure 3), especially around the centrilobular veins, or in the hepatic parenchyma such as the interlobular connective tissue or liver sinusoids. Dark brown dots, likely corresponding to aggregated nanomaterial, were found in the tissue 30 days after administration. The black arrow in Figure 3 depicts the recruitment of Kupffer cells in the liver 24 h after injection confirming the uptake by the reticuloendothelial system (RES) of the nanomaterial. Although their exact body absorption mechanism still needs further investigation, it is likely that the macrophages in the liver could gradually engulf the injected G-Rib, leading to its biodegradation. A possible explanation for the differences observed with the results of Sasidharan *et. al.*, could be that the method of exfoliation of graphene in the presence of riboflavin produces a more dispersible and stable nanomaterial compared with that obtained *via* arc discharge. This translates in a biological scenario into milder inflammatory responses and reduced general toxicity.

The spleen is the lymphoid organ involved in the filtration of blood and production of antibodies and activated lymphocytes, making it an important organ in the defense against antigens. Intravenous administration of FLG produced by arc discharge resulted in extensive spleen damage including the loss of the dividing line between red pulp and the marginal zone,

the abundance of megakaryocytes in the red pulp 90 days post injection, and a lack of lymphocytes in the white pulp.[43] In our H&E stained spleen slices from mice injected with G-Rib (Figure S1), we also noticed some dark brown spots, which, however, were relatively difficult to be differentiated from the stained nuclei of the spleen cells. Similar results were obtained by Yang et al., in a toxicity study with PEGylated nanographene sheets injected in a Balb/c animal model at 20 mg/kg.[48] Overall, G-Rib showed high accumulation in the mouse liver and possibly the spleen, which are RES organs responsible for the clearance of foreign materials by macrophage uptake. Moreover, as commented above, surface modification of FLG appears to be a key factor to reduce general toxicity. Those findings are in agreement with the reported biodistribution for other graphene related materials.[13,44]

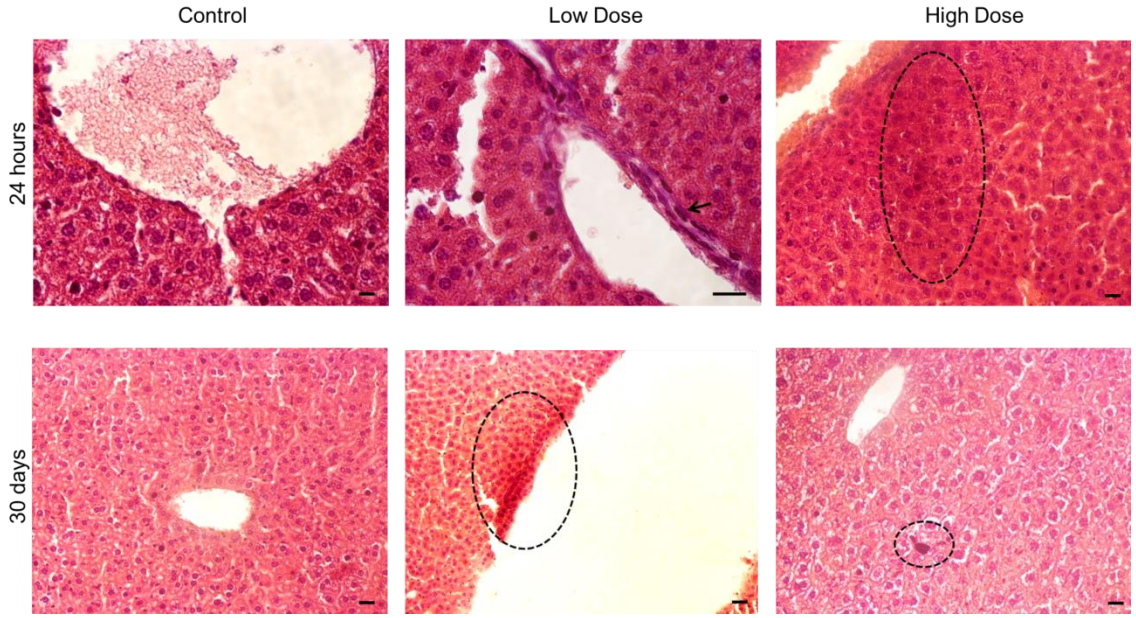

Figure 3. H&E staining of liver sections from control or G-Rib-treated mice (Low dose: 5 mg/kg body weight and high dose: 15 mg/kg body weight) at different times post-administration. Dotted-circles indicate possible nanomaterial accumulation in the tissue. The black arrow indicates the recruitment of Kupffer cells in the liver 24 h after injection. Scale bar: 20 μm.

Upon i.v. administration, nanomaterials could enter the kidneys through the renal artery and flow into the glomerular capillaries. Urinary excretion without affecting the glomerular structure is desirable for any nanomaterial intended for biomedical application.[54] This is why we further investigated whether graphene induced any damage to the kidneys' tissue. Previous

studies have described chronic interstitial nephritis caused by FLG after i.v. administration.[43] Authors described large numbers of darkly stained necrotic cells and dilation of tubules in FLG treated mice. After 24 hours post-administration, a significant darkening of the tissue was observed in the slices corresponding to the kidneys, which could be due to a transient deposition of G-Rib in these organs (Figure 4.). However, we could not find large aggregates suggesting no accumulation in this tissue. Furthermore, no organ damage or other structural changes were observed in all examined organs at any time point confirming our hypothesis that graphene exfoliation in presence of riboflavin can improve the biocompatibility of the nanomaterial. Future studies complementing histology must be carried out in order to elucidate the entire life cycle of G-Rib *in vivo*. Since FLG is a material without functional groups on the surface, it will be challenging to covalently attach markers to achieve radiolabeling for *in vivo* tracking of the material. This has been described before by Sasidharan et al., where FLG was excluded from the *in vivo* biodistribution analysis carried out in Swiss albino mice.[43] Instead, ex vivo analysis of the organs could be carried out on dehydrated tissue sections imaged under confocal Raman microscope, as reported by Syama et al., in a study for the detection of organ distribution and clearance of PEGylated reduced graphene oxide.[55] Finally, FLG hasn't shown damage on brain, heart, or testis in previous studies suggesting that material couldn't pass through the blood-brain barrier (BBB).[43] However, brain accumulation shows variable results across the literature. Whilst some authors have shown no accumulation or disruption of the BBB[51,56], an extensive review on the safety assessment of graphene-based materials summarizes different publications that have shown brain accumulation or a transitory decrease in the tightness of the blood–brain barrier.[6] A future study on the properties of G-Rib, exploring its biointeractions with the BBB and whether it can be delivered to such an important organ, should be explored.

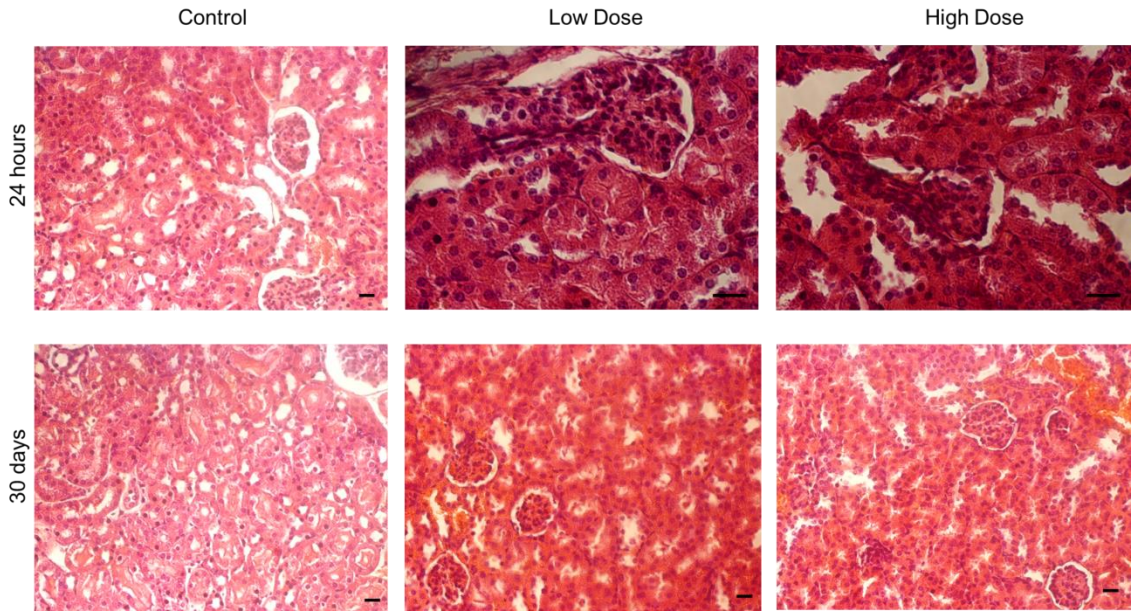

Figure 4. H&E staining of kidney sections from control or G-Rib-treated mice (Low dose: 5 mg/kg body weight and high dose: 15 mg/kg body weight) at different times post-administration. Scale bar: 20 μm.

3.5. Urine analysis

In order to characterize G-Rib clearance, urine was collected and analyzed by HR-TEM. For this purpose, urine was recovered from mice administered with the high dose of G-Rib and purified by dialysis in water to eliminate macromolecules and salts that may hamper the characterization by TEM. We were able to detect graphene sheets on the urine samples, analyzing the samples 18 hours after injection. (Figure 5a-b). A selected area electron diffraction analysis confirmed the crystalline nature of the sheet based on the typical six-fold symmetric diffraction spots for graphene (Figure 5c). This result indicates the possibility of urinary excretion of G-Rib, although it is impossible to state to what extent this material is eliminated in the urine. The total amount of graphene excreted in the urine was quantified when it was radiolabelled. For instance, in our previous work GO was covalently functionalized with DOTA allowing the chelation of ^{111}In or ^{64}Cu.[57,58] Other studies also reported the quantification of PEGylated graphene labelled with ^{125}I or GO with ^{188}Re.[44,45,48]

The renal journey of G-Rib was surprising, taking into account the restriction in size that the glomerular capillary wall imposes, where the functional or physiologic pore size is significantly smaller, measuring only 4.5-5 nm in diameter.[54] Nevertheless, carbon nanotubes with 20-30

nm in diameter were observed to pass through the glomerular barrier indicating that the filtration through the glomerular barrier is a complex process.[59] We hypothesize that the smallest and thinnest graphene sheets can certainly roll or fold during blood circulation allowing glomerular filtration and subsequent renal elimination.[11,60] This result is in agreement with other studies reporting the renal clearance of graphene materials.[57,58,61] For instance, we observed extensive urinary excretion of GO (lateral size dimension of the majority of the sheets < 1 μm).[11] Furthermore, as suggested by Russier *et al.*, another mechanism could be the sliding of the thin graphene sheets perpendicularly through the cellular membranes as observed *in vitro* and supported by *in silico* analysis.[62,63]

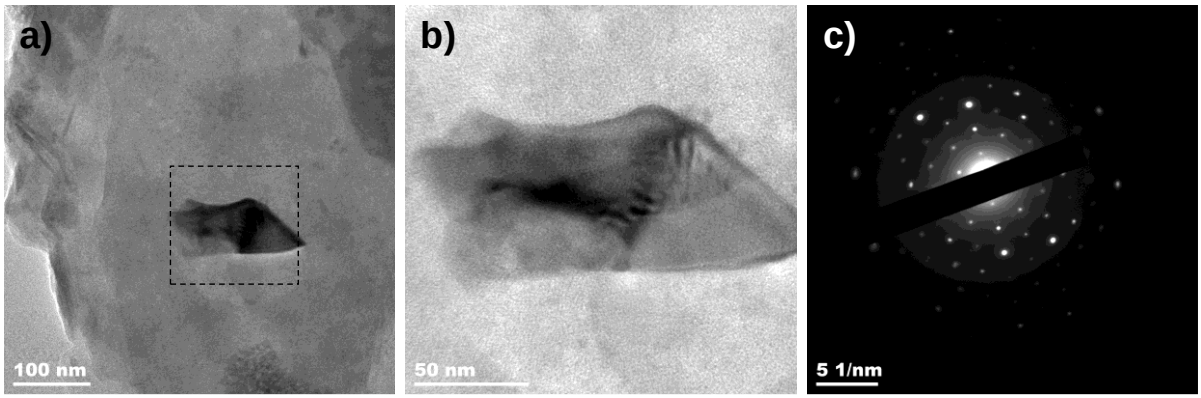

Figure 5: a) HR-TEM of G-Rib found in the urine of mice treated at the high dose (15 mg/kg body weight) of G-Rib. b) Magnified image on the selected area from panel a. c) SAED diffraction pattern corresponding to the structure observed.

3.6. Biochemical analyses

To assess the general toxicity of G-Rib, a complete biochemical analysis of blood samples was carried out after the intravenous administration of the material. Blood samples were collected at 24 h, 15 days and 30 days post-administration. The data is summarized in Table 1. Normal values across the study were obtained for the serum levels of AST, ALT, ALP, and creatinine as an expression of the correct function of the liver. Furthermore, normal levels of urea and creatinine confirmed no toxicological effects on renal function. FLG has been shown to cause a significant impact in classic hepatic and renal injury markers (e.g. the altered levels of AST, ALT and ALP over a period of 3 months, and high levels of blood urea nitrogen and creatinine).[43] Interestingly, our results suggest that the method of preparation of highly water

dispersible FLG using a biocompatible molecule like riboflavin could minimize FLG hepatic and renal injury.

Table 1. Clinical biochemical data obtained from control and experimental animals. The data shown represents the mean ± SD (n=5). Two-way ANOVA followed by Bonferroni's post-test: ns $p>0.05$, *$p<0.05$, **$p<0.01$, *** $p<0.001$ was used for statistical analysis.

	24 hours			15 days			30 days		
	Ctrl	**LD[a]**	**HD[a]**	**Ctrl**	**LD[a]**	**HD[a]**	**Ctrl**	**LD[a]**	**HD[a]**
Glucose (mmol/L)	13.50±1.41	12.22± 1.02	12.52± 2.81	11.95± 7.2	14.92± 2.34	8.65± 4.23	11.35± 4.17	10.87± 1.94	15.02± 2.52
Urea (mmol/L)	6.75± 0.49	6.25± 0.51	6.87± 0.76	6.9± 0.42	7.05± 0.78	7.625± 0.79	8.65± 0.07	6.35± 0.43	6.8± 1.09
Uric acid (µmol/L)	60.00± 4.24	74.25± 32.69	55.25± 26.84	144± 104.65	49± 17.75	259± 50.44	33.5± 19.09	35.5± 6.13	44.0± 14.62
Na (mmol/L)	144.5± 0.7	147± 3.55	145.3± 3.5	142± 8.48	147.5± 1.0	137.5± 1.73	149± 2.82	153.7± 4.57	150.5± 2.88
K (mmol/L)	4.80± 0.0	4.9± 0.33	4.7± 0.62	13.35± 12.09	4.7± 0.40	20.32± 0.95	4.15± 0.49	4.75± 0.56	4.35± 0.42
Cl (mmol/L)	107.5± 0.7	108.7± 1.25	106.5± 1.91	107± 4.24	109.5± 0.57	104.7± 1.70	112± 1.41	111.7± 1.70	108.7± 1.25
T. proteins (g/L)	49.00± 0.0	47.66± 2.51	47.33± 1.52	46.5± 3.53	45.0± 2.58	45.5± 2.51	50.0± 0.0	42.75± 3.20	45.5± 2.51
Albumin (g/L)	27.50± 0.7	26± 2.58	25.75± 2.21	28± 0.0	26.75± 0.95	27.5± 1.0	29.0± 0.0	21.25± 4.03	24.0± 2.58
Ca (mmol/L)	2.25± 0.07	2.25± 0.05	2.27± 0.12	2.25± 0.07	2.1± 0.08	2.07± 0.05	2.3± 0.14	2.3± 0.08	2.2± 0.0
P (mmol/L)	2.64± 0.44	2.3± 0.32	3.07± 0.99	2.64± 0.50	2.74± 0.54	3.12± 0.30	2.48± 0.38	2.145± 0.24	1.845± 0.31
Mg (mmol/L)	0.91± 0.09	0.85± 0.07	0.94± 0.18	1.135± 0.27	0.94± 0.13	1.28± 0.06	0.93± 0.14	0.895± 0.07	0.73± 0.10
Iron (µmol/L)	37.00± 4.24	32.75± 4.03	29± 3.55	49± 15.55	53.25± 6.13	32.25± 3.30	38.0± 4.24	25.5± 4.43	32.75± 2.87
T. bilirubin (µmol/L)	2.75± 0.07	2.57± 0.71	2.35± 0.66	3.1± 0.0	2.67± 0.23	-	1.4± 0.0	1.85± 0.1	1.57± 0.57
CK (U/L)	4361± 272.94	954± 579	2688± 1841	923± 0.0	1222±821.4	-	1343± 0.0	398± 254.2	190± 115.4
LDH (U/L)	1406± 251.73	879.3± 412.5	976.7± 452.9	1028± 0.0	683±146.5	-	688.0± 0.0	560.5± 83.25	329± 127.2
ASAT (U/L)	286.5± 16.26	157± 46.8	205.7± 104.05	143± 0.0	146.5± 41.55	-	160.0± 0.0	102.2± 20.10	74± 29.26
ALAT (U/L)	112.5± 36.06	69.33± 46.19	82± 39.64	161± 0.0	68.25± 30.5	31.33± 15.37	96.0± 35.35	56.75± 33.71	28.25± 9.03
ALP (U/L)	116.0± 1.41	100.3± 23.89	83.25± 23.41	135± 21.21	144± 1.15	117.7± 9.25	91.0± 15.55	53.5± 28.05	72.5± 19.13
α-Amylase (U/L)	645.0± 76.36	653.5± 46.04	580± 74.11	649.5± 91.21	652± 26.25	670± 104.61	718.5± 7.77	509.5± 87.20	673.2± 95.64
Glycerol (µmol/L)	511.0± 89.09	459.3± 27.1	437.3± 30.9	646.5± 26.16	688.3± 75.73	715.7± 93.65	573.5± 275.1	403± 201.73	531.5± 89.45

ƃ-HBA (µmol/L)	0.16± 0.07	0.16± 0.04	0.18± 0.03	0.275± 0.09	0.29± 0.01	0.135± 0.03	0.15± 0.042	0.155± 0.012	0.20± 0.08
Bile acids (µmol/L)	4.70± 0.98	9.86± 16.05	1.97± 1.10	4.25± 3.18	7.65± 2.80	3.55± 1.63	7.4± 6.08	2.8± 4.07	2.75± 4.04
Creatinine (µmol/L)	12.00± 0.0	11.0± 1.7	11.66± 1.15	12.5± 0.70	13± 2.0	13.5± 2.38	12± 0.0	11.25± 0.95	11.5± 1.29

[a] LD (low dose) corresponds to 5 mg/kg; HD (high dose) corresponds to 15 mg/kg.

To assess the hemocompatibility of G-Rib, selected hematological parameters were measured (Table 2). Most of all hematological parameters remained within the reference range showing no hematotoxicity compared to the control. Surprisingly, only the platelet counts showed a statistically significant higher value in the group treated with the low dose after 30 days of the injection. Activated platelets can act as pro-adhesive mediators for leukocytes, but since lymphocytes, granulocytes, and monocytes counts remained in the same range as the control we believe that this higher value is not a direct effect of the administration of G-Rib; which makes this material highly promising for biomedical applications through intravenous administration.

Several issues still need to be addressed. Further studies on the bio-interactions of G-Rib with other macromolecular components of the plasma, the formation of covalent or noncovalent protein corona, and the effect on the interaction with the surfactant, will further elucidate their impact on the stability, dispersibility, cell uptake, and, most importantly, the pharmacokinetics and pharmacodynamics of G-Rib. The relatively slow translation of graphene-based materials into clinical applications is their undetermined fate *in vivo*, which is revealed to be associated tightly with the protein corona effect formed immediately after administration.[64] This complex and dynamic process could be conducive to a gradual release of the molecules of riboflavin in the surface of the material that could be replaced by more thermodynamically favorable interactions with specific serum proteins. As showed by Huang *et al.*, in a study using all-atom molecular dynamics simulations, stability of mono-layer graphene with Rib is strongly dependent upon the amount of surfactant absorbed on the surface, showing that low or high concentrations lead to agglomeration and loss of stability in water.[65] However, the study did not investigate the interactions of G-Rib complex in the presence of other molecules or salt. Further studies *in silico* using molecular dynamics (MD) simulations, *in vitro*, and *in vivo* will help to understand adsorption profiles on G-Rib in a biological milieu and how we can control its pharmacokinetics and biodistribution.

Table 2. Hematological data obtained from control and experimental animals. The data shown represents the mean ± SD (n=5). Two-way ANOVA followed by Bonferroni's post-test: ns $p>0.05$, *$p<0.05$, **$p<0.01$, *** $p<0.001$ was used for statistical analysis.

	24 hours			15 days			30 days		
	Ctrl	**LD[a]**	**HD[a]**	**Ctrl**	**LD[a]**	**HD[a]**	**Ctrl**	**LD[a]**	**HD[a]**
WBC 10^3 cells/µL	7.47± 1.60	6.31± 1.46	8.73± 1.13	5.16± 0.13	6.17± 1.52	7.19± 0.76	3.74± 1.07	5.01± 1.00	8.73± 1.61
RBC 10^6 cells/µL	10.16± 0.42	9.53± 0.43	10.01± 0.15	10.07± 0.25	9.70± 0.54	10.05± 0.16	10.16± 0.20	8.35± 1.24	10.01± 0.45
HGB (g/dL)	14.70± 0.71	13.60± 0.87	14.40± 0.40	14.75± 0.35	13.68± 0.75	14.37± 0.15	14.50± 0.14	11.80± 1.84	14.40± 0.91
HCT (%)	49.70± 1.84	48.00± 1.73	49.40± 0.82	48.90± 1.56	48.20± 1.98	50.47± 1.17	50.50± 2.12	43.55± 5.42	49.40± 2.73
MCV (fL)	48.90± 0.28	50.37± 0.51	49.38± 1.13	48.55± 0.35	49.80± 1.11	50.27± 0.47	49.75± 1.06	52.35± 2.24	49.38± 0.67
MCH (pg)	14.50± 0.00	14.30± 0.26	14.35± 0.22	14.60± 0.00	14.10± 0.14	14.30± 0.10	14.35± 0.21	14.13± 0.24	14.35± 0.44
MCHC (g/dL)	29.60± 0.14	28.40± 0.79	29.15± 0.99	30.15± 0.21	28.38± 0.69	28.50± 0.36	28.80± 0.99	27.05± 1.55	29.15± 1.05
NEUTRO (%)	11.70± 1.13	27.27± 3.18	20.63± 5.77	15.60± 0.85	19.10± 5.78	21.93± 1.58	12.40± 0.99	33.08± 9.76	20.63± 4.62
LYMPHO (%)	82.10± 0.28	65.93± 3.52	73.15± 6.79	75.75± 2.76	75.63± 4.01	70.97± 3.70	75.80± 7.21	49.23± 18.30	73.15± 5.13
MONO (%)	3.25± 1.91	2.47± 0.61	1.65± 1.35	2.25± 0.07	1.55± 0.57	2.20± 0.75	1.40± 0.28	0.93± 0.58	1.65± 0.78
EOSINO (%)	2.50± 0.57	3.47± 1.16	3.23± 1.04	5.30± 2.12	2.53± 1.27	3.63± 2.06	9.55± 5.87	15.13± 8.66	3.23± 1.18
LUC (%)	0.35± 0.07	0.83± 0.35	1.25± 0.60	0.95± 0.35	1.08± 0.15	1.10± 0.10	0.80± 0.14	1.58± 0.69	1.25± 0.82
BASO (%)	0.10± 0.00	0.03± 0.06	0.10± 0.08	0.15± 0.07	0.13± 0.05	0.17± 0.06	0.10± 0.00	0.08± 0.05	0.10± 0.08
NEUTRO 10^3 cells/µL	0.92± 0.03	1.69± 0.27	1.77± 0.54	0.82± 0.00	1.16± 0.45	1.58± 0.12	0.44± 0.11	1.49± 0.53	1.77± 0.24
LYMPHO 10^3 cells/µL	6.48± 0.82	4.14± 1.05	6.48± 0.63	4.00± 0.35	4.57± 1.24	5.18± 0.91	2.73± 1.15	2.13± 0.67	6.48± 1.60
MONO 10^3 cells/µL	0.27± 0.18	0.16± 0.07	0.15± 0.13	0.12± 0.01	0.09± 0.05	0.16± 0.06	0.05± 0.01	0.04± 0.02	0.15± 0.08
EOSINO 10^3 cells/µL	0.20± 0.03	0.21± 0.02	0.28± 0.02	0.28± 0.10	0.15± 0.07	0.25± 0.11	0.31± 0.10	0.68± 0.40	0.28± 0.08
LUC 10^3 cells/µL	0.03± 0.01	0.05± 0.03	0.12± 0.05	0.05± 0.01	0.07± 0.01	0.08± 0.01	0.02± 0.00	0.07± 0.04	0.12± 0.08
BASO 10^3 cells/µL	0.00± 0.00	0.00± 0.00	0.01± 0.01	0.01± 0.00	0.01± 0.01	0.01± 0.00	0.00± 0.00	0.00± 0.00	0.01± 0.01
PLT 10^3 cells/µL	958.00± 90.51	1120± 144.02	1010.00 ±203.28	878.00 ±45.25	1094± 146.9	989± 113.4	897.0 ±120.2	1204*** ±394.8	1010± 439.2
MPV (fL)	4.10± 0.00	4.20± 0.00	4.65± 0.17	4.00± 0.14	4.00± 0.00	4.13± 0.15	4.60± 0.14	4.68± 0.31	4.65± 0.70

[a] LD (low dose) corresponds to 5 mg/kg; HD (high dose) corresponds to 15 mg/kg.

3.7. Immunofluorescence staining

Following the analysis of the injected mice, which showed normal behavior, we focused on the potential inflammatory reactions. Recent studies have shown that riboflavin presented an immunomodulatory effect in different *in vivo* studies (mice challenged with LPS, mice with induced peritonitis or acute lung injury).[66] However, those studies were carried out using riboflavin doses in the range of 20 to 100 mg/kg of body weight. In our study, the dispersion of G-Rib contains 7% weight of riboflavin. Mice injected with 100 or 300 µg of G-Rib will have a dose of riboflavin of 0.35 or 1.05 mg/kg of body weight, hence we believe that the use of riboflavin would not have a significant impact on the immunological response.

Lymph nodes and spleens were harvested, and grinded on a 100 µm strainer. The recovered cells were washed twice in PBS medium supplemented with 2% FBS and stained with fluorescently-labeled antibodies to evaluate the proportion of the different immune cell types and their activation status by flow cytometry, at the different time points and G-Rib i.v. administrated doses. Figure 6 displays the results of the immunophenotyping and the activation of the cells isolated from the lymph nodes. From the data gathered at 24 h after injection, no significant differences in immune cell proportion (~20% of B cells, ~80% T cells and <1% of macrophages and dendritic cells) nor in T or B cell activation (evaluated by CD69 or CD86 staining of both cell types) were seen. Despite the fact that at 15 and 30 days post-injection, we were able to see variations in B and total T cells (increase of B cells balanced by a decrease in T cells 30 days after injection, Figure 6D) from the mice injected with the low dose of graphene in comparison to the control mice, no real tendency to decrease or increase in activation seemed to emerge.

The same strategy was applied to the splenocytes (Figure 7), and in contrast to the lymph nodes, we noticed an increase of activation marker CD86 in macrophages for the mice injected with a high dose of G-Rib after 24 h (Figure 7B). This could point towards early signs of inflammation associated to the injection route, favoring an interaction of the material with splenocytes before affecting immune cells within the lymph nodes.[67] This situation appeared to be resolved at later time points, since the expression of activation markers was at the same level as the controls at 15 and 30 days after treatment in all the cell types (Figure 7D and 7F). Interestingly and as previously mentioned, the inflammatory phenotype was not observed at later time points in lymph nodes as could have been expected. It is worth to point out that similarly to the lymph nodes, a variation in the main immune cell populations (B and T cells) present in this secondary lymphoid organ could be observed as well. An impact (even indirect) of the G-Rib on

lymphocyte viability by induction of apoptosis could not be excluded as it has already been observed with other graphene-based material.[68] However, the $CD4^+$ T cells that were decreased at 15 days in the low dose injected mice, were rather increased 15 days later, suggesting a disruption followed by a recovery of lymphocyte homeostasis, reducing a potential G-Rib associated lymphopenia. Even though G-Rib seemed to affect lymphocyte proportions in both lymph nodes and the spleen, no obvious signs of increase in immune cell activation at late time points post-injection could be reported, suggesting no link between injections of either the low nor the high dose of FLG and long lasting inflammatory responses. It's noteworthy to mention that even when riboflavin has shown in recent studies an important role in the modulation of the immune response of the organism [66], in this study the activation level of the cells isolated from the lymph nodes and spleen did not show obvious signs of inflammation that could be associated to the injection of FLG.

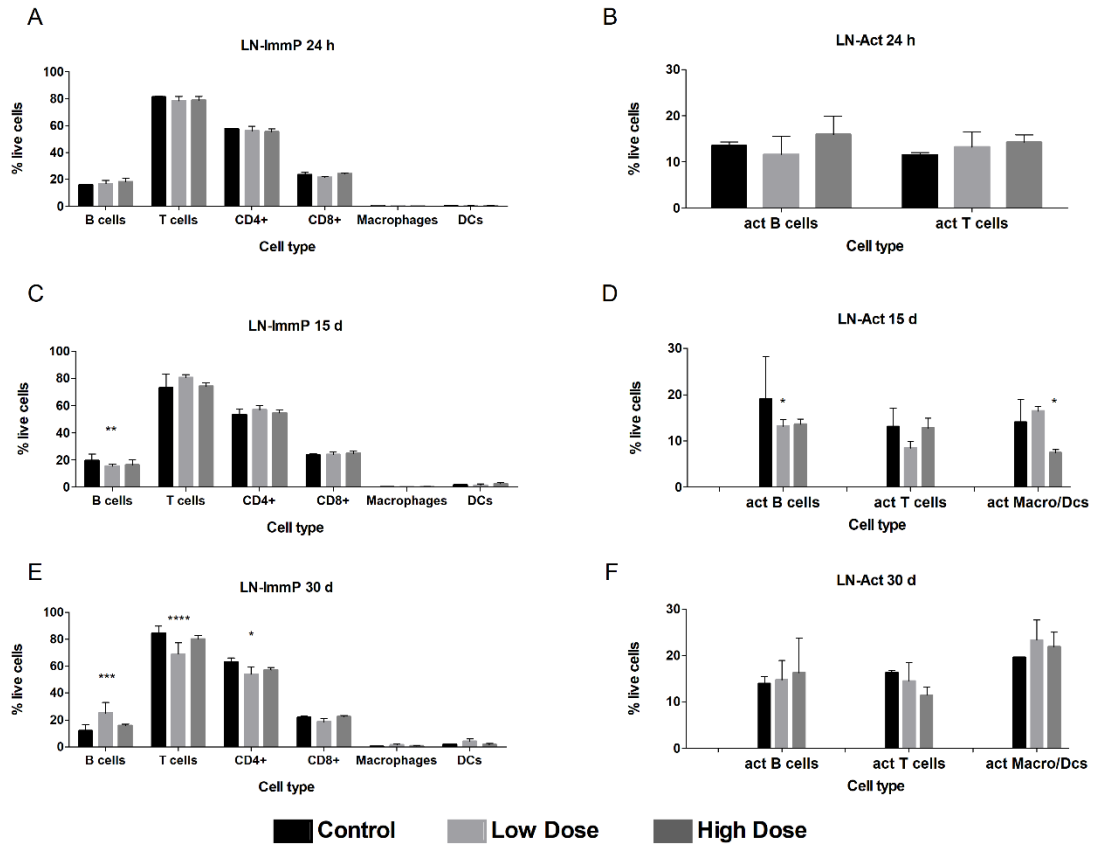

Figure 6. Cells isolated from lymph nodes of Balb/c mice at 24 hours, 15 days or 30 days post-injection with a 5% dextrose solution (control), a low or a high dose of graphene, were stained with (A, C, E) anti-mouse CD19, TCRβ, CD4, CD8, CD11b, and I^A-I^E to determine the proportion of B, T, $CD4^+$ and $CD8^+$ T cells, macrophages and dendritic cells (DCs) respectively.

To determine the immune cell activation, the gating was focused either on B, T cells or macrophages/DCs and evaluated for their expression of CD86 (B, D, F). Values represent the mean ± SD (n=5). Two-way ANOVA followed by Bonferroni's post-test: ns p>0.05, *p<0.05, **p<0.01, *** p<0.001 was used for statistical analysis.

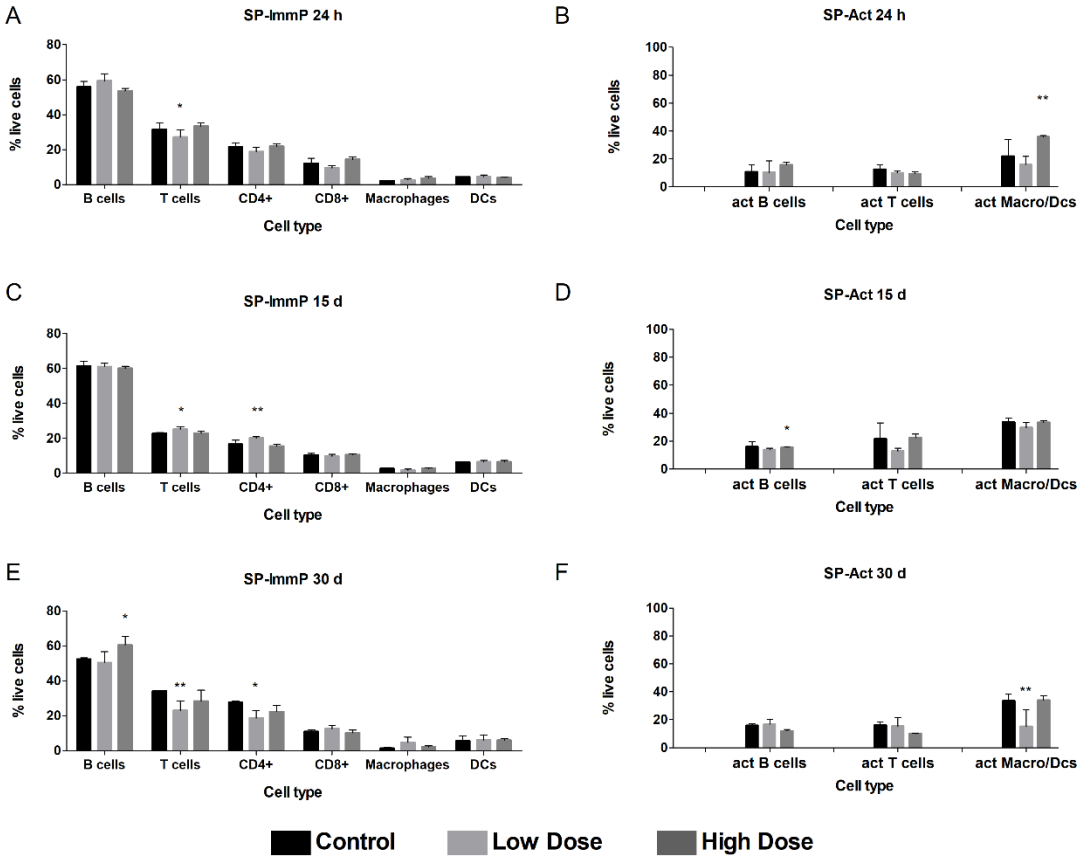

Figure 7. Cells isolated from the spleen of Balb/c mice, 24 h, 15 days or 30 days post-injection with a 5% dextrose solution (control), a low or a high dose of graphene, were stained with (A, C, E) anti-mouse CD19, TCRβ, CD4, CD8, CD11b and I^A-I^E to determine the proportion of B, T, $CD4^+$ and $CD8^+$ T cells, macrophages and dendritic cells respectively. To determine the immune cell activation, the gating was focused either on B, T cells or macrophages/DCs and evaluated for their expression of CD86 (B, D, F). Values represent the mean ± SD (n=5). Two-way ANOVA followed by Bonferroni's post-test: ns p>0.05, *p<0.05, **p<0.01, *** p<0.001 was used for statistical analysis.

4. Conclusions

The present study described the preparation of a stable and highly concentrated dispersion of graphene in aqueous media through a facile route of exfoliation using a biocompatible surfactant. The safety of the material was demonstrated *in vitro* and *in vivo*. Cell survival was above 85% in HeLa and RAW 264.7 cells across all concentrations studied and no morphological changes were observed 24 h after treatment. *In vivo* studies showed that biochemical and hematological parameters remained within the reference range showing no hematotoxicity compared to the control. Immunophenotyping and activation level of the cells isolated from the lymph nodes and spleen were also analyzed and no obvious signs of inflammation could be associated to the injection of either the low or the high dose of FLG. The transient activation of macrophages in the spleen after 24 h of injection and the detection of the material in the urine suggested a rapid and safe clearance, which is of utmost importance in the process to develop future biomedical applications and its translation into the clinic.

Acknowledgements

The authors gratefully acknowledge the financial support from the EU GRAPHENE Flagship project (no. 696656 and no. 785219), from the Agence Nationale de la Recherche (ANR) through the LabEx project Chemistry of Complex Systems (ANR-10-LABX-0026_CSC), through the program "Investissements d'Avenir" (ANR-11-EQPX-022), from the FLAG-ERA JTC 2015 G-IMMUNOMICS project (ANR-15-GRFL-0001-05), and from EU MSCA-RISE projet CARBO-IMmap (no. 734381). This work was partly supported by the Centre National de la Recherche Scientifique (CNRS), and the International Center for Frontier Research in Chemistry (icFRC). We also wish to acknowledge C. Royer and V. Demais for TEM analyses at the Plateforme Imagerie in Vitro at the Center of Neurochemistry (Strasbourg, France) and Dris Ihiawakrim for HR-TEM and SAED measurements.

References

[1] G. Reina, J.M. González-Domínguez, A. Criado, E. Vázquez, A. Bianco, M. Prato, Promises, facts and challenges for graphene in biomedical applications, Chem. Soc. Rev. (2017). https://doi.org/10.1039/c7cs00363c.

[2] I.A. Kinloch, J. Suhr, J. Lou, R.J. Young, P.M. Ajayan, Composites with carbon nanotubes and graphene: An outlook, Science (80-.). 362 (2018) 547–553. https://doi.org/10.1126/science.aat7439.

[3] E. Masvidal-Codina, X. Illa, M. Dasilva, A.B. Calia, T. Dragojević, E.E. Vidal-Rosas, E. Prats-Alfonso, J. Martínez-Aguilar, J.M. De la Cruz, R. Garcia-Cortadella, P. Godignon, G. Rius, A. Camassa, E. Del Corro, J. Bousquet, C. Hébert, T. Durduran, R. Villa, M. V. Sanchez-Vives, J.A. Garrido, A. Guimerà-Brunet, High-resolution mapping of infraslow cortical brain activity enabled by graphene microtransistors, Nat. Mater. 18 (2019) 280–288. https://doi.org/10.1038/s41563-018-0249-4.

[4] N. Panwar, A.M. Soehartono, K.K. Chan, S. Zeng, G. Xu, J. Qu, P. Coquet, K.-T. Yong, X. Chen, Nanocarbons for Biology and Medicine: Sensing, Imaging, and Drug Delivery, Chem. Rev. (2019) acs.chemrev.9b00099. https://doi.org/10.1021/acs.chemrev.9b00099.

[5] M.O. Ansari, K. Gauthaman, A. Eissa, S.A. Bencherif, A. Memic, Graphene and graphene-based materials in biomedical applications, Curr. Med. Chem. 26 (2019). https://doi.org/10.2174/0929867326666190705155854.

[6] B. Fadeel, C. Bussy, S. Merino, E. Vázquez, E. Flahaut, F. Mouchet, L. Evariste, L. Gauthier, A.J. Koivisto, U. Vogel, C. Martín, L.G. Delogu, T. Buerki-Thurnherr, P. Wick, D. Beloin-Saint-Pierre, R. Hischier, M. Pelin, F. Candotto Carniel, M. Tretiach, F. Cesca, F. Benfenati, D. Scaini, L. Ballerini, K. Kostarelos, M. Prato, A. Bianco, Safety Assessment of Graphene-Based Materials: Focus on Human Health and the Environment, ACS Nano. 12 (2018) 10582–10620. https://doi.org/10.1021/acsnano.8b04758.

[7] L. Ou, B. Song, H. Liang, J. Liu, X. Feng, B. Deng, T. Sun, L. Shao, Toxicity of graphene-family nanoparticles: A general review of the origins and mechanisms, Part. Fibre Toxicol. 13 (2016) 57. https://doi.org/10.1186/s12989-016-0168-y.

[8] M. Ema, M. Gamo, K. Honda, A review of toxicity studies on graphene-based nanomaterials in laboratory animals, Regul. Toxicol. Pharmacol. 85 (2017) 7–24. https://doi.org/10.1016/J.YRTPH.2017.01.011.

[9] G. Reina, A. Ruiz, D. Murera, Y. Nishina, A. Bianco, "Ultramixing": A Simple and Effective Method To Obtain Controlled and Stable Dispersions of Graphene Oxide in Cell Culture Media, ACS Appl. Mater. Interfaces. 11 (2019) 7695–7702. https://doi.org/10.1021/acsami.8b18304.

[10] A.F. Rodrigues, L. Newman, D.A. Jasim, I.A. Vacchi, C. Ménard-Moyon, L.E. Crica, A. Bianco, K. Kostarelos, C. Bussy, Immunological impact of graphene oxide sheets in the abdominal cavity is governed by surface reactivity, Arch. Toxicol. 92 (2018) 3359–3379. https://doi.org/10.1007/s00204-018-2303-z.

[11] D.A. Jasim, S. Murphy, L. Newman, A. Mironov, E. Prestat, J. McCaffrey, C. Ménard-Moyon, A.F. Rodrigues, A. Bianco, S. Haigh, R. Lennon, K. Kostarelos, The Effects of Extensive Glomerular Filtration of Thin Graphene Oxide Sheets on Kidney Physiology, ACS Nano. 10 (2016) 10753–10767. https://doi.org/10.1021/acsnano.6b03358.

[12] L. Mao, M. Hu, B. Pan, Y. Xie, E.J. Petersen, Biodistribution and toxicity of radio-labeled few layer graphene in mice after intratracheal instillation, Part. Fibre Toxicol. 13 (2015) 7. https://doi.org/10.1186/s12989-016-0120-1.

[13] M. Amrollahi-Sharifabadi, M.K. Koohi, E. Zayerzadeh, M.H. Hablolvarid, J. Hassan, A.M. Seifalian, In vivo toxicological evaluation of graphene oxide nanoplatelets for clinical application, Int. J. Nanomedicine. Volume 13 (2018) 4757–4769. https://doi.org/10.2147/IJN.S168731.

[14] A. Schinwald, F.A. Murphy, A. Jones, W. MacNee, K. Donaldson, Graphene-Based Nanoplatelets: A New Risk to the Respiratory System as a Consequence of Their Unusual Aerodynamic Properties, ACS Nano. 6 (2012) 736–746. https://doi.org/10.1021/nn204229f.

[15] E.-J. Park, S.J. Lee, K. Lee, Y.C. Choi, B.-S. Lee, G.-H. Lee, D.-W. Kim, Pulmonary persistence of graphene nanoplatelets may disturb physiological and immunological homeostasis, J. Appl. Toxicol. 37 (2017) 296–309. https://doi.org/10.1002/jat.3361.

[16] S. Jaworski, B. Strojny, E. Sawosz, M. Wierzbicki, M. Grodzik, M. Kutwin, K. Daniluk, A. Chwalibog, S. Jaworski, B. Strojny, E. Sawosz, M. Wierzbicki, M. Grodzik, M. Kutwin, K. Daniluk, A. Chwalibog, Degradation of Mitochondria and Oxidative Stress as the Main Mechanism of Toxicity of Pristine Graphene on U87 Glioblastoma Cells and Tumors and HS-5 Cells, Int. J. Mol. Sci. 20 (2019) 650. https://doi.org/10.3390/ijms20030650.

[17] M. Pelin, L. Fusco, C. Martín, S. Sosa, J. Frontiñán-Rubio, J.M. González-Domínguez, M. Durán-Prado, E. Vázquez, M. Prato, A. Tubaro, Graphene and graphene oxide induce ROS production in human HaCaT skin keratinocytes: the role of xanthine oxidase and NADH dehydrogenase, Nanoscale. 10 (2018) 11820–11830. https://doi.org/10.1039/C8NR02933D.

[18] M. Ayán-Varela, J.I. Paredes, L. Guardia, S. Villar-Rodil, J.M. Munuera, M. Díaz-González, C. Fernández-Sánchez, A. Martínez-Alonso, J.M.D. Tascón, Achieving Extremely Concentrated Aqueous Dispersions of Graphene Flakes and Catalytically Efficient Graphene-Metal Nanoparticle Hybrids with Flavin Mononucleotide as a High-Performance Stabilizer, ACS Appl. Mater. Interfaces. 7 (2015) 10293–10307. https://doi.org/10.1021/acsami.5b00910.

[19] N. Beztsinna, M. Solé, N. Taib, I. Bestel, Bioengineered riboflavin in nanotechnology, Biomaterials. 80 (2016) 121–133. https://doi.org/10.1016/j.biomaterials.2015.11.050.

[20] M. Darguzyte, N. Drude, T. Lammers, F. Kiessling, Riboflavin-Targeted Drug Delivery, Cancers (Basel). 12 (2020) 295. https://doi.org/10.3390/cancers12020295.

[21] M. Lotya, Y. Hernandez, P.J. King, R.J. Smith, V. Nicolosi, L.S. Karlsson, F.M. Blighe, S. De, W. Zhiming, I.T. McGovern, G.S. Duesberg, J.N. Coleman, Liquid phase production of graphene by exfoliation of graphite in surfactant/water solutions, J. Am. Chem. Soc. 131 (2009) 3611–3620. https://doi.org/10.1021/ja807449u.

[22] M. Cai, D. Thorpe, D.H. Adamson, H.C. Schniepp, Methods of graphite exfoliation, J. Mater. Chem. 22 (2012) 24992–25002. https://doi.org/10.1039/c2jm34517j.

[23] J.M. González-Domínguez, V. León, M. Isabel Lucío, M. Prato, E. Vázquez, Production of ready-to-use few-layer graphene in aqueous suspensions, Nat. Publ. Gr. 13 (2018). https://doi.org/10.1038/nprot.2017.142.

[24] A. Bianco, H.M. Cheng, T. Enoki, Y. Gogotsi, R.H. Hurt, N. Koratkar, T. Kyotani, M. Monthioux, C.R. Park, J.M.D. Tascon, J. Zhang, All in the graphene family - A recommended nomenclature for two-dimensional carbon materials, Carbon N. Y. 65 (2013) 1–6. https://doi.org/10.1016/j.carbon.2013.08.038.

[25] A. Ciesielski, P. Samorì, Graphene via sonication assisted liquid-phase exfoliation, Chem. Soc. Rev. 43 (2014) 381–398. https://doi.org/10.1039/c3cs60217f.

[26] Z. Sun, J. Masa, Z. Liu, W. Schuhmann, M. Muhler, Highly concentrated aqueous dispersions of graphene exfoliated by sodium taurodeoxycholate: Dispersion behavior and potential application as a catalyst support for the oxygen-reduction reaction, Chem. - A Eur. J. 18 (2012) 6972–6978. https://doi.org/10.1002/chem.201103253.

[27] F. Bonaccorso, L. Colombo, G. Yu, M. Stoller, V. Tozzini, A.C. Ferrari, R.S. Ruoff, V. Pellegrini, Graphene, related two-dimensional crystals, and hybrid systems for energy conversion and storage, Science (80-.). 347 (2015) 1246501. https://doi.org/10.1126/science.1246501.

[28] G. Shim, M.G. Kim, J.Y. Park, Y.K. Oh, Graphene-based nanosheets for delivery of chemotherapeutics and biological drugs, Adv. Drug Deliv. Rev. (2016). https://doi.org/10.1016/j.addr.2016.04.004.

[29] Y. Cao, The Toxicity of Nanoparticles to Human Endothelial Cells, in: Q. Saquib, M. Faisal, A.A. Al-Khedhairy, A.A. Alatar (Eds.), Springer International Publishing, Cham, 2018: pp. 59–69. https://doi.org/10.1007/978-3-319-72041-8_4.

[30] D. Murera, S. Malaganahalli, C. Martín, G. Reina, J.-D. Fauny, H. Dumortier, E. Vázquez, A. Bianco, Few layer graphene does not affect the function and the autophagic activity of primary lymphocytes, Nanoscale. 11 (2019) 10493–10503. https://doi.org/10.1039/C9NR00846B.

[31] S. Malanagahalli, D. Murera, C. Martín, H. Lin, N. Wadier, H. Dumortier, E. Vázquez, A. Bianco, Few Layer Graphene Does Not Affect Cellular Homeostasis of Mouse Macrophages, Nanomaterials. 10 (2020) 228. https://doi.org/10.3390/nano10020228.

[32] C. Liao, Y. Li, S. Tjong, Graphene Nanomaterials: Synthesis, Biocompatibility, and Cytotoxicity, Int. J. Mol. Sci. 19 (2018) 3564. https://doi.org/10.3390/ijms19113564.

[33] I.O. for Standardization, I.O. for Standardization, ISO 10993-5: Biological evaluation

of medical devices-Part 5: Tests for in vitro cytotoxicity, (2009).

[34] A.M. Pinto, I.C. Gonçalves, F.D. Magalhães, Graphene-based materials biocompatibility: A review, Colloids Surfaces B Biointerfaces. 111 (2013) 188–202. https://doi.org/10.1016/J.COLSURFB.2013.05.022.

[35] S. Gurunathan, J.-H. Kim, Synthesis, toxicity, biocompatibility, and biomedical applications of graphene and graphene-related materials, Int. J. Nanomedicine. 11 (2016) 1927. https://doi.org/10.2147/IJN.S105264.

[36] G. Lalwani, M. D'Agati, A.M. Khan, B. Sitharaman, Toxicology of graphene-based nanomaterials, Adv. Drug Deliv. Rev. 105 (2016) 109–144. https://doi.org/10.1016/J.ADDR.2016.04.028.

[37] A. Sasidharan, L.S. Panchakarla, P. Chandran, D. Menon, S. Nair, C.N.R. Rao, M. Koyakutty, Differential nano-bio interactions and toxicity effects of pristine versus functionalized graphene, Nanoscale. 3 (2011) 2461. https://doi.org/10.1039/c1nr10172b.

[38] K.-H. Liao, Y.-S. Lin, C.W. Macosko, C.L. Haynes, Cytotoxicity of Graphene Oxide and Graphene in Human Erythrocytes and Skin Fibroblasts, ACS Appl. Mater. Interfaces. 3 (2011) 2607–2615. https://doi.org/10.1021/am200428v.

[39] Y. Li, Y. Liu, Y. Fu, T. Wei, L. Le Guyader, G. Gao, R.-S. Liu, Y.-Z. Chang, C. Chen, The triggering of apoptosis in macrophages by pristine graphene through the MAPK and TGF-beta signaling pathways, Biomaterials. 33 (2012) 402–411. https://doi.org/10.1016/J.BIOMATERIALS.2011.09.091.

[40] L. Farcal, F.T. Andón, L. Di Cristo, B.M. Rotoli, O. Bussolati, E. Bergamaschi, A. Mech, N.B. Hartmann, K. Rasmussen, J. Riego-Sintes, J. Ponti, A. Kinsner-Ovaskainen, F. Rossi, A. Oomen, P. Bos, R. Chen, R. Bai, C. Chen, L. Rocks, N. Fulton, B. Ross, G. Hutchison, L. Tran, S. Mues, R. Ossig, J. Schnekenburger, L. Campagnolo, L. Vecchione, A. Pietroiusti, B. Fadeel, Comprehensive in vitro toxicity testing of a panel of representative oxide nanomaterials: First steps towards an intelligent testing strategy, PLoS One. (2015). https://doi.org/10.1371/journal.pone.0127174.

[41] M.C. Duch, G.R.S. Budinger, Y.T. Liang, S. Soberanes, D. Urich, S.E. Chiarella, L.A.

Campochiaro, A. Gonzalez, N.S. Chandel, M.C. Hersam, G.M. Mutlu, Minimizing Oxidation and Stable Nanoscale Dispersion Improves the Biocompatibility of Graphene in the Lung, Nano Lett. 11 (2011) 5201–5207. https://doi.org/10.1021/nl202515a.

[42] I. Dudek, M. Skoda, A. Jarosz, D. Szukiewicz, The Molecular Influence of Graphene and Graphene Oxide on the Immune System Under In Vitro and In Vivo Conditions, Arch. Immunol. Ther. Exp. (Warsz). 64 (2016) 195–215. https://doi.org/10.1007/s00005-015-0369-3.

[43] A. Sasidharan, S. Swaroop, C.K. Koduri, C.M. Girish, P. Chandran, L.S. Panchakarla, V.H. Somasundaram, G.S. Gowd, S. Nair, M. Koyakutty, Comparative in vivo toxicity, organ biodistribution and immune response of pristine, carboxylated and PEGylated few-layer graphene sheets in Swiss albino mice: A three month study, Carbon N. Y. 95 (2015) 511–524. https://doi.org/10.1016/j.carbon.2015.08.074.

[44] X. Zhang, J. Yin, C. Peng, W. Hu, Z. Zhu, W. Li, C. Fan, Q. Huang, Distribution and biocompatibility studies of graphene oxide in mice after intravenous administration, Carbon N. Y. 49 (2011) 986–995. https://doi.org/10.1016/j.carbon.2010.11.005.

[45] S. Zhang, K. Yang, L. Feng, Z. Liu, In vitro and in vivo behaviors of dextran functionalized graphene, Carbon N. Y. 49 (2011) 4040–4049. https://doi.org/10.1016/j.carbon.2011.05.056.

[46] J.-H. Liu, S.-T. Yang, H. Wang, Y. Chang, A. Cao, Y. Liu, Effect of size and dose on the biodistribution of graphene oxide in mice, Nanomedicine. 7 (2012) 1801–1812. https://doi.org/10.2217/nnm.12.60.

[47] K. Yang, S. Zhang, G. Zhang, X. Sun, S.-T. Lee, Z. Liu, Graphene in Mice: Ultrahigh In Vivo Tumor Uptake and Efficient Photothermal Therapy, Nano Lett. 10 (2010) 3318–3323. https://doi.org/10.1021/nl100996u.

[48] K. Yang, J. Wan, S. Zhang, Y. Zhang, S.-T. Lee, Z. Liu, In Vivo Pharmacokinetics, Long-Term Biodistribution, and Toxicology of PEGylated Graphene in Mice, ACS Nano. 5 (2011) 516–522. https://doi.org/10.1021/nn1024303.

[49] S. Kanakia, J. Toussaint, D.M. Hoang, S. Mullick Chowdhury, S. Lee, K.R. Shroyer, W. Moore, Y.Z. Wadghiri, B. Sitharaman, Towards An Advanced Graphene-Based

Magnetic Resonance Imaging Contrast Agent: Sub-acute Toxicity and Efficacy Studies in Small Animals, Sci. Rep. 5 (2015) 17182. https://doi.org/10.1038/srep17182.

[50] S.M. Chowdhury, S. Kanakia, J.D. Toussaint, M.D. Frame, A.M. Dewar, K.R. Shroyer, W. Moore, B. Sitharaman, In Vitro Hematological and In Vivo Vasoactivity Assessment of Dextran Functionalized Graphene, Sci. Rep. 3 (2013) 2584. https://doi.org/10.1038/srep02584.

[51] S. Kanakia, J.D. Toussaint, S. Mullick Chowdhury, T. Tembulkar, S. Lee, Y.-P. Jiang, R.Z. Lin, K.R. Shroyer, W. Moore, B. Sitharaman, Dose ranging, expanded acute toxicity and safety pharmacology studies for intravenously administered functionalized graphene nanoparticle formulations, Biomaterials. 35 (2014) 7022–7031. https://doi.org/10.1016/j.biomaterials.2014.04.066.

[52] N. Kurantowicz, B. Strojny, E. Sawosz, S. Jaworski, M. Kutwin, M. Grodzik, M. Wierzbicki, L. Lipińska, K. Mitura, A. Chwalibog, Biodistribution of a High Dose of Diamond, Graphite, and Graphene Oxide Nanoparticles After Multiple Intraperitoneal Injections in Rats, Nanoscale Res. Lett. 10 (2015) 398. https://doi.org/10.1186/s11671-015-1107-9.

[53] K.M. Tsoi, S.A. MacParland, X.-Z. Ma, V.N. Spetzler, J. Echeverri, B. Ouyang, S.M. Fadel, E.A. Sykes, N. Goldaracena, J.M. Kaths, J.B. Conneely, B.A. Alman, M. Selzner, M.A. Ostrowski, O.A. Adeyi, A. Zilman, I.D. McGilvray, W.C.W. Chan, Mechanism of hard-nanomaterial clearance by the liver, Nat. Mater. 15 (2016) 1212–1221. https://doi.org/10.1038/nmat4718.

[54] M. Longmire, P.L. Choyke, H. Kobayashi, Clearance properties of nano-sized particles and molecules as imaging agents: considerations and caveats, Nanomedicine. 3 (2008) 703–717. https://doi.org/10.2217/17435889.3.5.703.

[55] S. Syama, W. Paul, A. Sabareeswaran, P.V. Mohanan, Raman spectroscopy for the detection of organ distribution and clearance of PEGylated reduced graphene oxide and biological consequences, Biomaterials. 131 (2017) 121–130. https://doi.org/10.1016/j.biomaterials.2017.03.043.

[56] K. Wang, J. Ruan, H. Song, J. Zhang, Y. Wo, S. Guo, D. Cui, Biocompatibility of Graphene Oxide, Nanoscale Res Lett. 6 (2010) 8. https://doi.org/10.1007/s11671-010-

9751-6.

[57] D.A. Jasim, C. Ménard-Moyon, D. Bégin, A. Bianco, K. Kostarelos, Tissue distribution and urinary excretion of intravenously administered chemically functionalized graphene oxide sheets, Chem. Sci. 6 (2015) 3952–3964. https://doi.org/10.1039/C5SC00114E.

[58] D.A. Jasim, H. Boutin, M. Fairclough, C. Ménard-Moyon, C. Prenant, A. Bianco, K. Kostarelos, Thickness of functionalized graphene oxide sheets plays critical role in tissue accumulation and urinary excretion: A pilot PET/CT study, Appl. Mater. Today. 4 (2016) 24–30. https://doi.org/10.1016/j.apmt.2016.04.003.

[59] R. Singh, D. Pantarotto, L. Lacerda, G. Pastorin, C. Klumpp, M. Prato, A. Bianco, K. Kostarelos, Tissue biodistribution and blood clearance rates of intravenously administered carbon nanotube radiotracers, Proc. Natl. Acad. Sci. 103 (2006) 3357–3362. https://doi.org/10.1073/pnas.0509009103.

[60] N. Patra, B. Wang, P. Král, Nanodroplet Activated and Guided Folding of Graphene Nanostructures, Nano Lett. 9 (2009) 3766–3771. https://doi.org/10.1021/nl9019616.

[61] C. Gómez-Navarro, J.C. Meyer, R.S. Sundaram, A. Chuvilin, S. Kurasch, M. Burghard, K. Kern, U. Kaiser, Atomic Structure of Reduced Graphene Oxide, Nano Lett. 10 (2010) 1144–1148. https://doi.org/10.1021/nl9031617.

[62] J. Russier, E. Treossi, A. Scarsi, F. Perrozzi, H. Dumortier, L. Ottaviano, M. Meneghetti, V. Palermo, A. Bianco, Evidencing the mask effect of graphene oxide: a comparative study on primary human and murine phagocytic cells, Nanoscale. 5 (2013) 11234. https://doi.org/10.1039/c3nr03543c.

[63] R. Guo, J. Mao, L.-T. Yan, Computer simulation of cell entry of graphene nanosheet, Biomaterials. 34 (2013) 4296–4301. https://doi.org/10.1016/j.biomaterials.2013.02.047.

[64] X. Lu, P. Xu, H.-M. Ding, Y.-S. Yu, D. Huo, Y.-Q. Ma, Tailoring the component of protein corona via simple chemistry, Nat. Commun. 10 (2019) 4520. https://doi.org/10.1038/s41467-019-12470-5.

[65] S. Huang, A. Croy, V. Bezugly, G. Cuniberti, Stabilization of aqueous graphene dispersions utilizing a biocompatible dispersant: a molecular dynamics study, Phys.

Chem. Chem. Phys. 21 (2019) 24007–24016. https://doi.org/10.1039/C9CP04742E.

[66] N. Suwannasom, I. Kao, A. Pruß, R. Georgieva, H. Bäumler, Riboflavin: The Health Benefits of a Forgotten Natural Vitamin, Int. J. Mol. Sci. 21 (2020) 950. https://doi.org/10.3390/ijms21030950.

[67] S.L. Sheasley-O'Neill, C.C. Brinkman, A.R. Ferguson, M.C. Dispenza, V.H. Engelhard, Dendritic Cell Immunization Route Determines Integrin Expression and Lymphoid and Nonlymphoid Tissue Distribution of CD8 T Cells, J. Immunol. 178 (2007) 1512–1522. https://doi.org/10.4049/jimmunol.178.3.1512.

[68] L. Ou, S. Lin, B. Song, J. Liu, R. Lai, L. Shao, The mechanisms of graphene-based materials-induced programmed cell death: a review of apoptosis, autophagy, and programmed necrosis, Int. J. Nanomedicine. Volume 12 (2017) 6633–6646. https://doi.org/10.2147/IJN.S140526.